Dipartimento di Fisica e Astronomia Galileo Galilei

1222·2022 800 ANNI

Università degli Studi di Padova

Measurement of the critical temperature of a superconductor via Meissner effect

Matteo De Tullio - 1225015 - matteo.detullio@studenti.unipd.it
Arianna Mischianti - 1236935 - arianna.mischianti@studenti.unipd.it
Pierpaolo Ranieri - 1225016 - pierpaolo.ranieri@studenti.unipd.it

(Dated: March 19, 2021)

The aim of this laboratory activity is to study and analyze the behavior of a ceramic superconductor below its critical temperature. Nowadays it is a known fact that, under such a condition, superconductors show remarkable features: they exhibit zero resistivity and a perfect diamagnetism (Meissner effect). The superconducting specimen was inserted inside a coil whose inductance value is measured through an amplifying resonant circuit. At the critical temperature the sample becomes diamagnetic; as a consequence, the magnetic field flux lines are expelled from the coil inside, causing a decrease in the inductance, which leads to an increase in the resonant frequency of the oscillating circuit.

CONTENTS

I. INTRODUCTION

The intent of this section is to provide a general idea about the main features of a superconducting material. Going through the most remarkable discoveries the aim is to give some insights on the main physical properties, paying particular attention to the *Meissner effect*. Demonstrating its experimental evidence will be useful in the following, as it is necessary to reach our goal, i.e. the measurement of the critical temperature T_C of an unknown superconductor specimen. Ultimately, the knowledge of this parameter will conduct to the identification of the sample.

1. The superconductivity phenomenon: main discoveries, theories and experimental evidences

Superconductivity is a physical phenomenon which was discovered in 1911 by H. K. Onnes, as he studied the properties of metals at low temperatures. On measuring the resistance of a small tube filled with mercury, he observed that its resistance fell from $\approx 0.1\ \Omega$ at a temperature of 4.3 K to less than $3 \times 10^{-6}\ \Omega$ at 4.1 K. The temperature below which the mercury becomes superconducting is known as its **critical temperature** T_C.

In 1933 W. Meissner and R. Ochsenfeld discovered that superconductors are also characterized by the important property of expelling a magnetic field from their inside. However, the field is ejected only if its intensity is below a certain *critical value*, depending on the material, the temperature and the geometry of the sample. Above that critical intensity, superconductivity disappears. Fritz and Heinz London were the first to propose a model describing the expulsion of the field in 1935.

The quantum theory of superconductivity was the BCS, published in 1957 by J. Bardeen, L. Cooper and J. Schrieffer. According to their theory, there is an attractive interaction between electrons in the superconducting state, mediated by the vibrations of the ion lattice. A consequence of this interaction is that electrons are paired together into a macroscopic quantum state, called *condensate*, which extends along the superconductor.

By the early 1960s there had been major advances in superconductor technology, with the discovery of alloys that were superconducting at temperatures higher than the critical temperatures of the elemental superconductors.

The aim was to discover a material that could undergo the superconducting transition at the temperature of liquid nitrogen (77.4 K), in such a way that all costs associated with the use of liquid helium for cooling could be avoided, making applications of superconductivity more economically worthwhile.

A turning point was, in 1986, when G. Bednorz and A. Muller discovered that **ceramics** made of Barium, Lanthanum, Copper and Oxygen (LBCO) became superconducting at 30 K, the highest known critical temperature at that time. Finally, in 1987, P. Chu produced a new ceramic material by replacing Lanthanum by Yttrium (YBCO), and found that it had a critical temperature of 90 K. This great jump in the critical temperature made it possible to use liquid nitrogen as a coolant.

Unfortunately, no superconductors have yet been found with critical temperatures close to room temperature, so **cryogenic cooling** is still a vital part of any superconducting application.

2. Properties of superconductors

The most evident feature of a superconductor is the complete disappearance of its resistivity below a temperature that is known as its critical temperature. On the other hand, in presence of a *normal conductor*, it is possible to observe that resistivity gradually decreases until reaching a certain value ρ_0 when approaching the absolute zero temperature. This behaviour is shown in figure 1.
The intensity of the magnetic field is directly proportional to the current flowing through a superconducting loop. By measuring the field intensity, it is possible to evaluate these currents without drawing energy from the circuit, as it would happen, instead, if placing an amperometer into it.
Until now the experimental results showed that the magnetic field has always remained constant within the precision of the measuring equipment, putting in evidence that a persistent current is an intrinsic feature of the superconducting state.

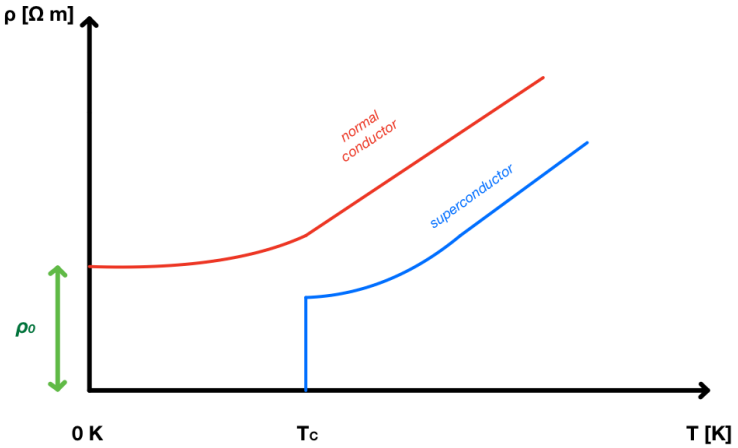

FIG. 1 Comparison between trends of resistivity as a function of the material temperature for a *normal conductor* and a *superconductor*, where T_C is the critical temperature and ρ_0 is the asymptotic value of the resistivity for a normal conductor at $T = 0$.

An important consequence of the persistent currents that flow in materials with zero resistivity is that the magnetic flux that passes through a continuous loop of such a material remains constant.

A. The Meissner Effect

The *Meissner Effect* is a physical phenomenon, which is observable for every superconductor. It is proven that, in presence of an external magnetic field with a lower intensity with respect to a certain critical value, every superconductor becomes perfectly *diamagnetic*, expelling the magnetic field lines from its inside.

The expulsion of the magnetic field from a superconductor takes place regardless of whether the sample becomes superconducting before or after the external magnetic field is applied. This occurs through the generation of surface currents which induce, inside the superconductor, a magnetic field opposite to the applied one.

The expulsion of the magnetic field from inside a superconductor cannot be predicted by applying Maxwell's equations to a material that has zero electrical resistance. Hence, in order to clear up how the Meissner Effect works, it is useful to distinguish a perfect conductor from a superconductor. For a perfect conductor, which has no resistance, the following expression holds:

$$0 = I \cdot R = V_{em} = \int_\Sigma (\nabla \times \mathbf{E}) \cdot d\mathbf{\Sigma} = -\frac{\partial}{\partial t} \int_\Sigma \mathbf{B} \cdot d\Sigma \longrightarrow \frac{\partial \Phi_B}{\partial t} = 0 \tag{1}$$

This implies that there is no temporal variation for the flux of the magnetic field.

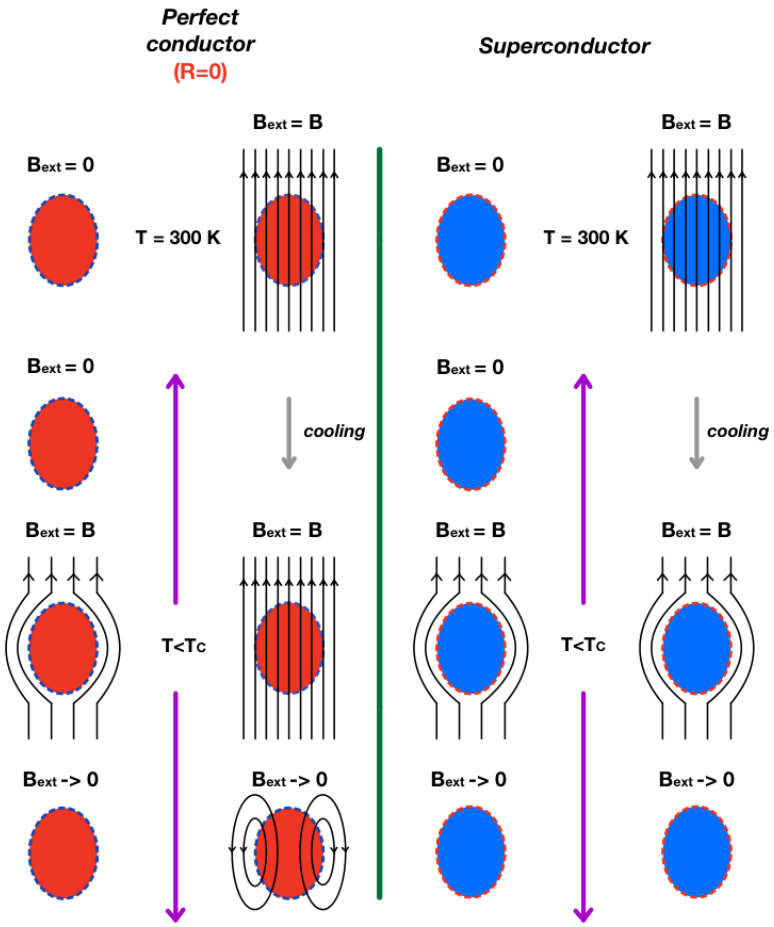

FIG. 2 Comparison between the responses offered respectively by a perfect conductor (on the left) and a superconductor (on the right) to an external applied magnetic field.

In a zero magnetic field environment, a perfect conductor is cooled below the temperature at which its resistance becomes zero. When a magnetic field is applied from the outside, screening currents are induced on the surface to keep the field at null value within the material. When the external field is switched off, the internal magnetic field stays at zero.
Cooling a perfect conductor below its critical temperature in a uniform magnetic field leads to a situation where the uniform field is maintained within the material. If the applied field is then removed, the field within the conductor stays uniform, due to the fact that the magnetic flux does not vary. These conditions are shown on the left side of the figure 2.

On the other hand, referring to a superconductor, if it is cooled below its critical temperature within either a zero magnetic field or a finite one, its intensity inside the material will be always zero. This is achieved spontaneously by the formation of currents on the surface of the superconductor. The direction of the currents is such to create a magnetic field that exactly cancels the applied field from the outside. It is this active exclusion of magnetic field the distinctive element of a superconductor in contrast to what happens for a perfect conductor. The superconductor response can be observed on the right side of figure 2.

3. Types of superconductors

Superconductors can be classified according to different criteria. One of those is their way of responding to an external applied magnetic field. More in detail, a division can be made into two main categories:

- **Type I** - These superconductors show a single critical value for the magnetic field, beyond which its lines are

entirely expelled outside.

- **Type II** - In this case there are two critical values, between which a partial penetration of the magnetic field is allowed through certain isolated points, called *vortexes*.

Another classification can be operated depending on the critical temperature of the superconductor. Hence, the main distinction is between *low temperature* ($T_C < 30\,K$) and *high temperature* ($T_C > 30\,K$) superconductors. Actually, high temperature superconductors can be chosen based on their ability to complete the transition when only cooled using liquid nitrogen at 77.4 K. This feature is relevant from an experimental point of view, as liquid nitrogen is a widespread coolant and in general because it is easier to control the temperature keeping it that low.

4. Experimental method

In order to accomplish the experiment's aim, it is necessary to link the reaching of the critical temperature T_C to the occurrence of the Meissner effect. This is a smart way to avoid the insertion of direct ohmic contacts, which could affect the sample integrity (it is a fragile material).
The proposed way to verify the expulsion of magnetic field is inserting the superconducting sample inside a coil, which is part of a selective amplifier. Its resonant frequency f_0 will depend on the inductance L of the coil according to the following relation:

$$f_0 = \frac{1}{2\pi\sqrt{LC}} \tag{2}$$

The inductance value is directly proportional to the flux of the internal magnetic field ϕ_B:

$$L = \frac{\phi_B}{i} \tag{3}$$

where i is the current passing through the coil.
When the magnetic flux lines start to be expelled from the superconductor, due to the Meissner effect, the flux inside the coil drops, so it is expected to observe a lowering of the inductance L, which brings to an increase of f_0 of the circuit.

II. EXPERIMENTAL APPARATUS

1. The Wheatstone bridge

The Wheatstone bridge is an electrical circuit, whose utility is to measure an unknown electrical resistance. In this analysis it was built in order to measure the temperature of our sample. For this purpose a Pt100 thermometer was used; it is a platinum sensor, through which it is possible to convert accurately resistance measurements into temperature ones. A convenient version of the Wheatstone bridge for the experiment's goal could be the three wire bridge, since it allows the electrical connection between the Pt100 and the rest of the circuit through three wires of resistance r. The described configuration is shown in figure **3**.
The Wheatstone bridge can be *balanced* by canceling the potential difference between A and B points, V_{AB}, in the circuit mentioned before. By applying that condition, it is possible to link the thermometer resistance R_T to the knob-controlled resistor R_X:

$$V_{AB} = 0 \implies R_T = R_X \tag{4}$$

To choose the other two resistances, R_1 and R_2, which need to be equal, it is necessary to impose a condition over the total power dissipated on the Pt100, which has to be 10^{-4} W, in order not to generate an additional source of heat inside the vacuum chamber in the next part of the experiment. The three-wire bridge was powered by an AC

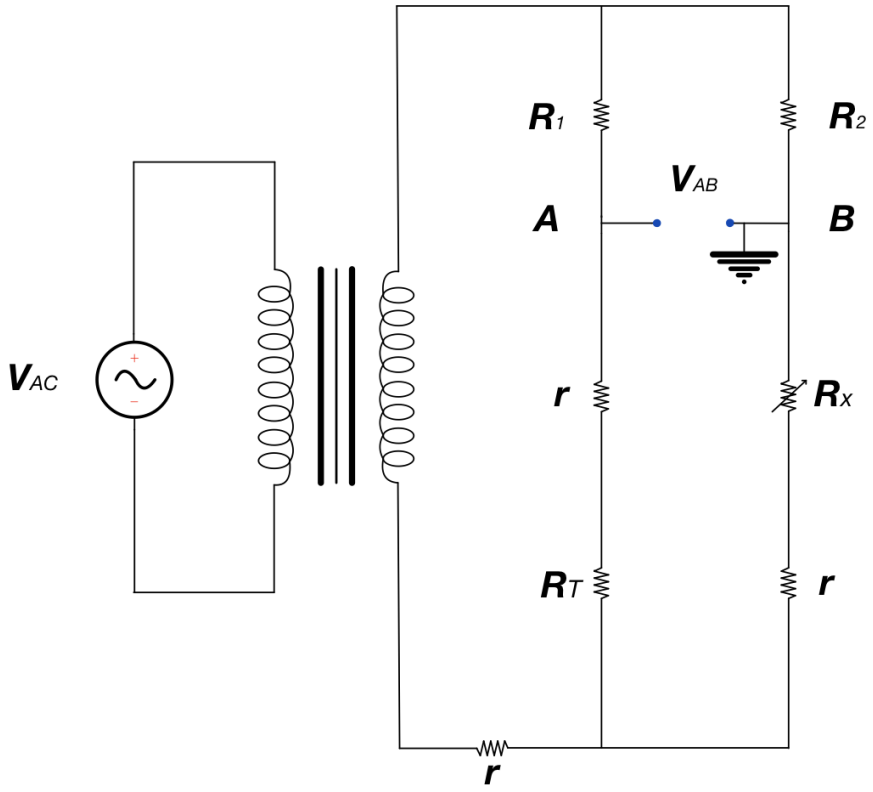

FIG. 3 Scheme of the Wheatstone bridge.

sinusoidal signal of frequency $f = 30$ Hz, so the current circulating into the circuit depends on the time according to the expression:

$$i(t) = i_0\, sen(\omega t) \qquad \text{with} \qquad \omega = 2\pi f \tag{5}$$

The power dissipated on a resistor by Joule heating is:

$$P(t) = R_{\text{tot}}\, i^2(t) = R_{\text{tot}}\, i_0^2\, sen^2(\omega t) \qquad \text{where} \qquad R_{\text{tot}} = R_T + R_1 \tag{6}$$

So the maximum power dissipated is:

$$P_{\max} = R_{\text{tot}} i_0^2 = \frac{V_{0P}^2}{R_{\text{tot}}} \tag{7}$$

where $V_{0P} = R_{\text{tot}} i_0$ is the signal amplitude from a zero value to the peak one, provided by the function generator. The power dissipated on the thermometer resistance is:

$$P_{\max} = R_T i_0^2 = R_T \frac{V_{0P}^2}{(R_T + R_1)^2} \leq 10^{-4}\text{W} \tag{8}$$

since we know that R_T varies inside the interval [0, 100] Ω, the condition for the resistance is:

$$R_1 \geq \sqrt{\frac{R_T}{10^{-4}}} V_{0P} - R_T \tag{9}$$

Thus, using an input voltage $V_{0P} = 2.5$ V the result is:

$$R \geq 2.4\,\text{k}\Omega$$

We have chosen values for the resistors $R_1 = R_2 = 14.99 \pm 0.14$ kΩ, which abundantly satisfies the condition just illustrated. We can avoid to consider the three wire resistances r, since they are negligible with respect to R_T.

2. Selective resonant amplifier

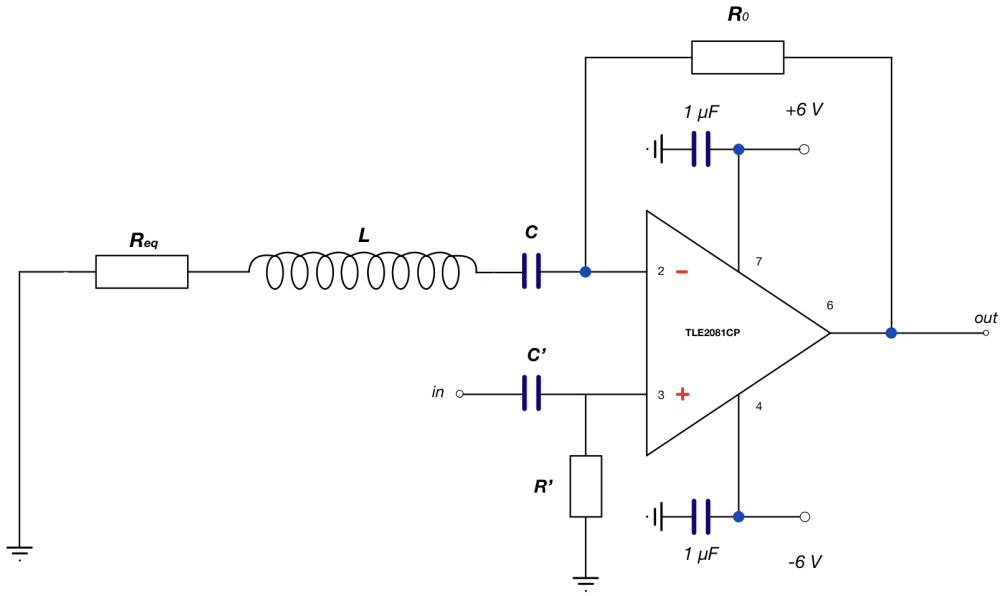

FIG. 4 Scheme of the selective amplifier adopted, equipped with a *high-pass RC filter*.

For the measurement of the coil inductance L, a selective resonant amplifier was designed as shown in figure 4. The goal was to perform a non-inverting amplifier in order to have a resonant frequency of 100 kHz and a gain of 100. To obtain such a gain, it was taken into account the fact that the RLC circuit configuration has an equivalent resistance of $R_{eq} = R_{coil} = 10.0 \pm 0.3\ \Omega$ (neglecting the wires resistance r'), the gain formula for a non-inverting amplifier becomes:

$$G = 1 + \frac{R_0}{R_{eq}} = 1 + \frac{R_0}{R_{coil} + r'} \simeq 1 + \frac{R_0}{R_{coil}} \tag{10}$$

Exploiting this relation, it was found that a resistor of 0.99 kΩ was needed. It was finally chosen a resistance of value $R_0 = 1.00 \pm 0.01$ kΩ.
As required, the employed circuit must amplify signals with a certain frequency of the order of $\simeq 100$ kHz, which is the reason why a selective amplifier is needed. To be able to set it to 100 kHz the value of C must be appropriately chosen such that the equation 2 is satisfied.

An operational amplifier TLE2081CP was used in the realization of the selective circuit, therefore the technical limits of the latter were taken into consideration: the amplitude of the output voltage must be lower than the maximum value of ±12 V and the product of resonant frequency and gain (GBP) must be less than 9.4 MHz.
The power supply was of ±6 V; the pins were connected to ground by means of two capacitors of 1 μF, with the scope of stabilizing the signal. The high pass filter in the lower branch was not built because a preliminary study described in section **III.2** was performed to prove that the resonance curve is already very narrow, so there is no need to cut off the lower frequencies. The resulting new selective circuit is shown in the following figure 5:

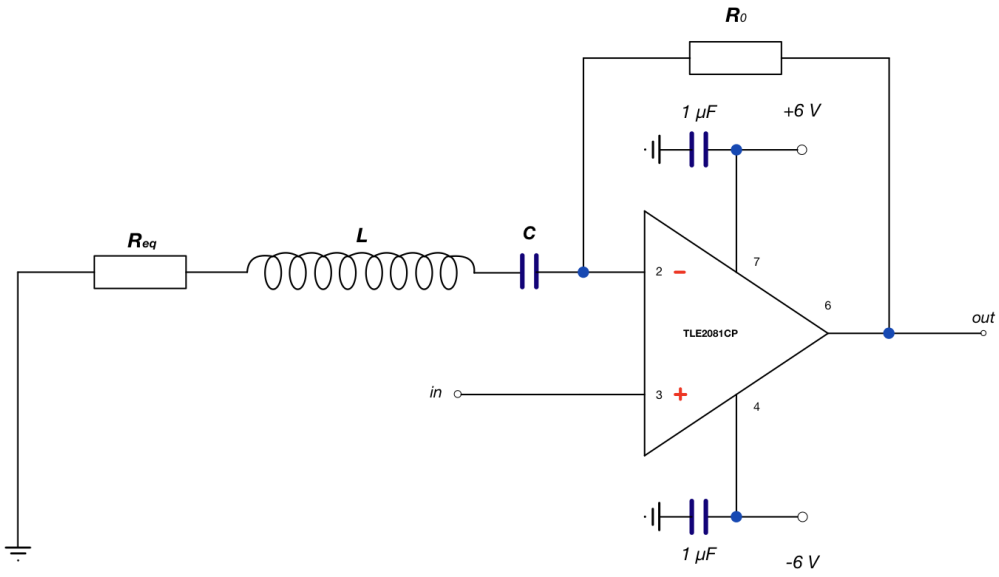

FIG. 5 Scheme of the previous selective amplifier, but in this case getting rid of the RC filter.

A sinusoidal input signal was given by the function generator Tektronix AFG3021, of $V_{\text{pp}} = 29.8 \pm 0.9$ mV and variable frequency.

3. Vacuum and cooling apparatus

The experimental apparatus, including the vacuum chamber, can be observed in figure 6.
The vacuum chamber is tightly anchored around the second stage of a cryocooler with a vacuum flange sealed with a O-ring. The chamber has multiple ports, covered with vacuum flanges, which allow to install the electric wires and the pump inside the walls of the chamber.
A high vacuum condition was achieved through a rotary pump; in this way a very low pressure value was obtained inside the chamber in a short time.
Using a Pirani gauge the pressure value reached inside the chamber was measured, obtaining, after a certain amount of time, a value almost constant in time of $p = 10^{-4}$ mbar.
Using a cryocooler the sample temperature was lowered. By means of the Pt100 thermometer, secured with a screw to the cold finger of the cryocooler, it was possible to check its temperature during the cooling phase.
The Pt100 thermometer was connected to an Arduino board interfaced with a dedicated LabView program through which it was possible to visualize the recorded temperature values in real time as a function of the Arduino output voltage. The sample rate of the Arduino was $f_{\text{sampling}} \simeq 1$ Hz.
In order to ensure the cooling down of the superconductor inside the sample holder, some precautions have been taken. The sample holder was tightly fixed to the cold finger using screws and grease in order to reduce the thermal insulation due to the presence of air between the two parts. In addition to that, the ceramic sample must be thermally connected with the sample holder. For this purpose some thin aluminum sheets have been inserted to fill the empty spaces inside the cylindrical support, and then the same operation was performed in the space between the cylindrical support and the sample holder. Another Pt100 thermometer was fixed with a screw upon the sample holder near the sample to control any possible differences in temperature between the cryocooler and the sample itself.
A resistor heater CAL-R 50 Ω was attached to the sample. This component could be connected to a feedback system and its aim was to heat the sample faster to make more measurements.

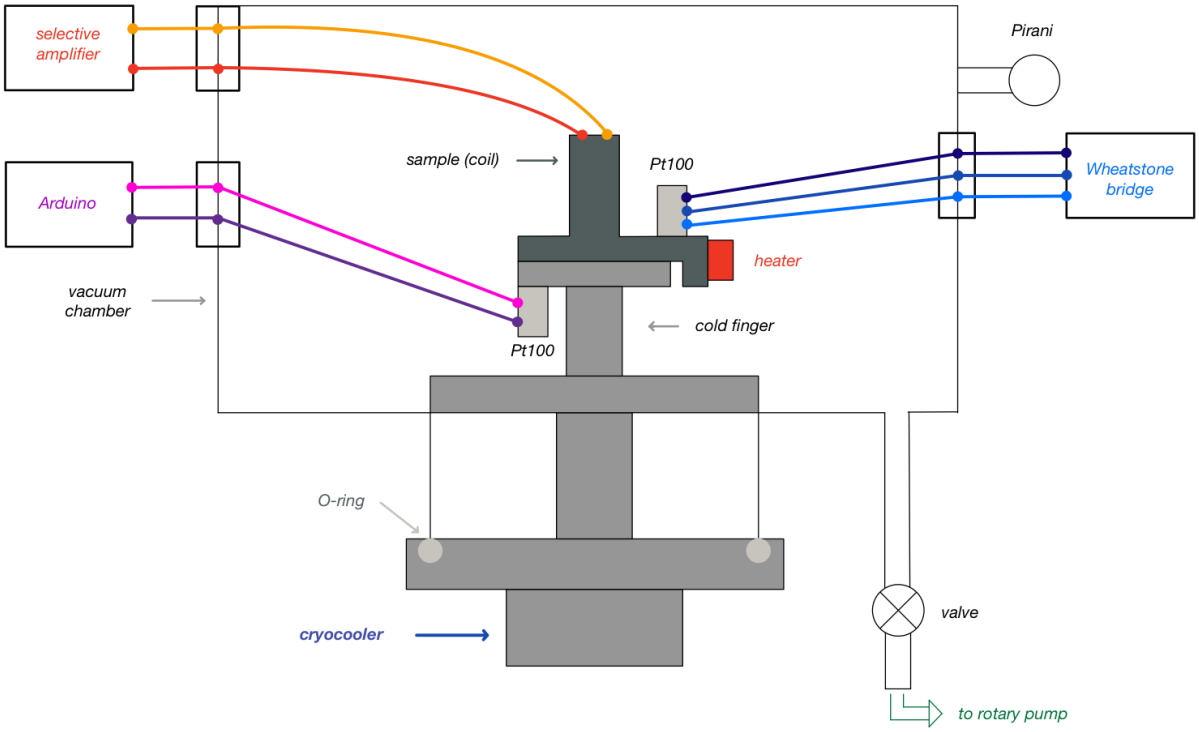

FIG. 6 Scheme of the vacuum chamber.

III. EXPERIMENTAL PROCEDURE

1. The Wheatstone bridge

The final configuration of the Wheatstone bridge displayed in figure 3 was achieved step by step. The first one was to perform a DC configuration (figure 7) to understand how much reliable is the reading of the potentiometer resistor. This is an important preliminary check to make sure that the associated value of the temperature is the real one.
Some resistors were chosen to be compared to the potentiometer resistance. Its resistance value was varied by turning the knob, until a continuous signal of zero voltage, $V_{AB} = 0$, was found. A perfect match was experienced between the helipot and the chosen resistors.

Switching to the AC connection that is found in figure 8, a sinusoidal function of $\simeq 30$ Hz was provided from the function generator. The oscilloscope was then connected to the A-B points and, after having set the bridge to the equilibrium condition, a sinusoidal voltage signal V_{AB} of amplitude $V_{\text{pp}} = 312 \pm 9$ mV was observed.

Later on, the A-B poles position was inverted and the voltage was measured once again. In this case, it was observed that the variation of the potentiometer resistance value does not produce changes in the voltage amplitude. This is explained by the fact that both the oscilloscope and the function generator are connected to a common ground. Consequently, according to the implemented oscilloscope connection, either the resistance R_T (fig. 8 - *right*) or the helipot (fig. 8-*left*) are short-circuited. In fact while turning the knob, no variation was actually observed.
In both cases a part of the circuit is excluded; to solve this problem the two grounds must be decoupled. To do this, a transformer 1:1 was used to isolate the generator ground. This structure is able to provide a signal, having a fixed frequency of 30 Hz, whose amplitude can be varied by means of another helipot. The signal was set to $V_{\text{pp}} = 5.0 \pm 0.2$ V. With this new configuration (figure 3) the grounds of the circuit are successfully isolated and varying the helipot resistance around the value of the chosen trial resistor (to be placed instead of R_T), a signal V_{AB}, variable in amplitude, was visualized, with a minimum of $V_{AB}^{\text{equilib.}} = 216 \pm 6$ mV.

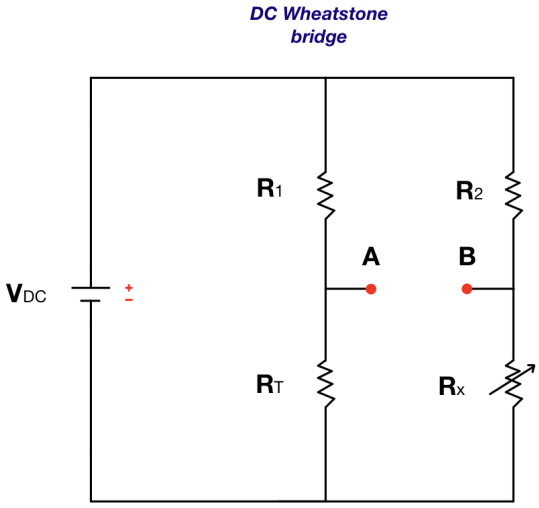

FIG. 7 Preliminary DC circuits.

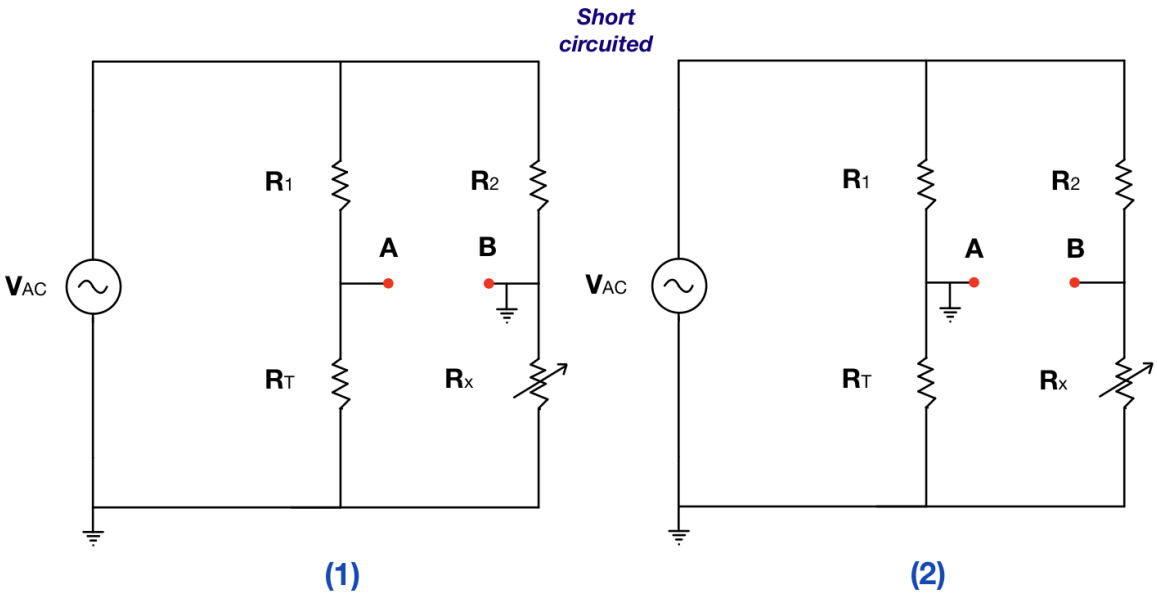

FIG. 8 Preliminary AC circuits.

2. Selective resonant amplifier

The coil, which constitutes the inductance of our circuit, was made by rolling a copper wire around a suitable cylindrical support. In this phase, it was paid attention to produce homogeneous layers of copper, trying to prevent any possibility of overlaps of the wire from occurring. In this way, rolling the copper wire by hand for each turn, a total of 500 turns were made.
Since our secondary purpose is to find the inductance experimentally, a theoretical value should be taken into account. The value of the inductance can be calculated using the geometric parameters of the coil according to the formula:

$$L = \frac{\mu N^2 \pi r_C^2}{l} \tag{11}$$

where μ is the magnetic permeability of the medium inside the coil, N is the number of coils, r_C is the radius of

the cylinder, in which the coil can be wrapped, and l the length of the cylinder.
The radius of the solenoid is not easy to determine, due to the presence of overlapping layers. Therefore, using a caliper, two measures were taken. As it can be seen in figure 9 before rolling the copper wire, the diameter of the cylindrical support, which stands for the diameter of the smallest layer of coils ($\simeq 70$ coils), was estimated, and after the accomplishment of rolling process, the diameter of the largest layer of coils were measured. In this way the coil can be modeled as one with 500 turns with the same radius, given by the mean of the two measured radii.

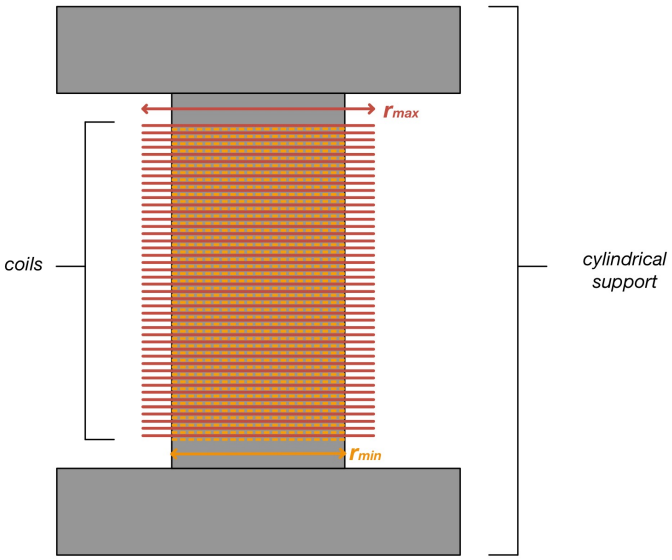

FIG. 9 Scheme of the coil.

It was obtained a value of $r_C = 3.2 \pm 0.1$ mm and of $l = 14.8 \pm 0.1$ mm. Thus, a value of $L = 0.68 \pm 0.04$ mH was found.
A capacitor, which is suitable to have a resonant frequency of 100 kHz, is expected to have a capacitance of $\simeq 4$ nF. On top of that, to understand if this is the best choice to obtain a narrow resonance peak a preliminary study was performed out of the vacuum chamber with different values for the capacitors.

Starting from $C = 1$ nF, the resonant frequency has been evaluated from the oscilloscope case by case. With this purpose, the two channels of the oscilloscope were respectively connected to the signal delivered by the function generator and to the output signal of the selective amplifier. It is expected to find a signal with maximum gain corresponding to the resonant frequency. By varying the frequency of the signal provided by the function generator, it is possible to detect a variation in the output amplitude, and this corresponds to a change in gain, since $G = V_{out}/V_{in}$. By setting the frequency in such a way to obtain the maximum voltage amplitude, and therefore the maximum gain, the resonance condition was achieved. The results are displayed in table 1.

C (nF)	$\simeq f_0$ (kHz)
1.0 ± 0.2	207
4.7 ± 0.3	94
10.0 ± 0.3	65
22.0 ± 0.4	42

TAB. 1 Resonant frequency for different capacitors.

As it can be seen, the values of C which allowed to reach a resonant frequency as close as possible to the value of 100 kHz were 4.7 nF and 10 nF. Thus, the resonance curves for these two values of C were performed. As a fact, by changing capacitor, leaving the same resistors, a shift of the curves along the frequency axis occurred. It was decided to plot the G/G_0 trend as a function of f/f_0, normalized to make the two curves comparable.
By superposition of the two graphs in figure 10, it was possible to make a comparison between them and therefore

to choose the capacitance which would have produced the best performance for our circuit. Since the two curves are very similar each other, regarding the narrowness of the peak, the employed capacitor is the one that allows to reach the closest frequency to 100 kHz value, which is the slightly narrower one in the figure. Hence the $C = 4.7 \pm 0.3$ nF capacitor was the right one.

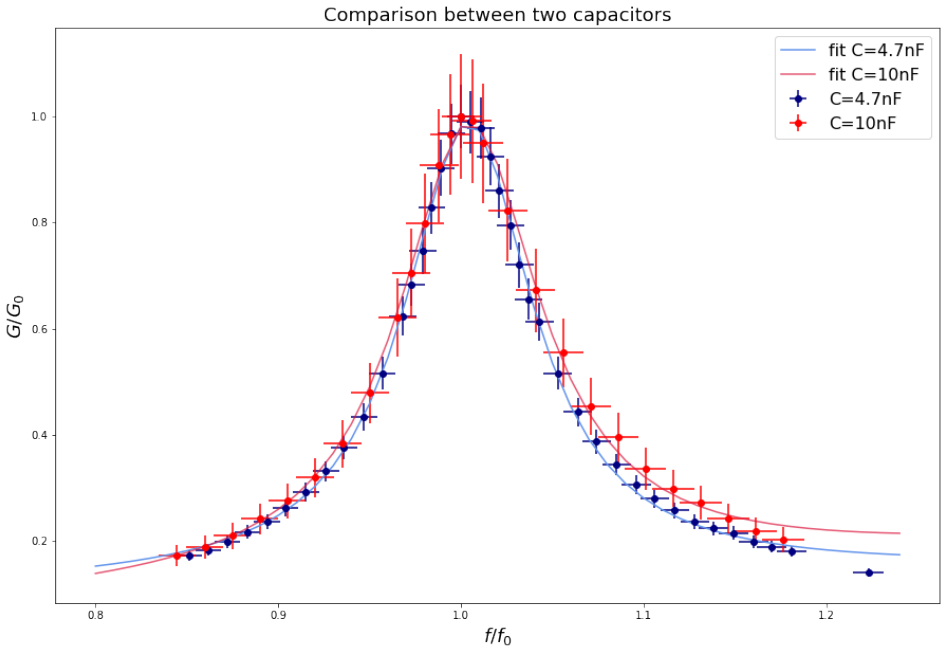

FIG. 10 Trends for the normalized gain as a function of the normalized frequencies. A Lorentzian fit was performed on both curves to identify the resonant frequency and the maximum gain.

The resonance curves are fitted with a Lorentzian function:

$$G(f) = \frac{A}{1 + \left(\frac{f - f_0}{B}\right)^2} + b \tag{12}$$

Using this formula it was possible to estimate the resonant frequency and the maximum gain, that in the selected configuration are respectively $f_0 = 94.38 \pm 0.04$ kHz and $G_{max} = 47 \pm 3$. This allowed to compute the resistance of the wires, knowing the maximum gain and the selected resistor:

$$r' = \frac{R_0}{G_{max} - 1} - R_{coil} \tag{13}$$

with a result of $r' = 11.8 \pm 0.3\ \Omega$. As it can be seen, the resistance of the wires has the same order of magnitude of R_{coil}, and it cannot be neglected. In the next part of the experiment, high resistance wires were used, hence it is expected to find a lower maximum gain.

3. Vacuum and cooling apparatus

As a preliminary check of the correctness of the apparatus designed so far, the superconducting condition was achieved using liquid nitrogen. In this way the superconductor should manifest the Meissner effect. The sample should eject the magnetic field generated by the coil from its inside and the inductance should drop. Thus a new value is obtained, as mentioned in section I.4.

A lowering of L, using the same capacitor, leads to an higher resonant frequency. A preliminary rough estimate of the resonant frequency leads to a shift of ~ 9 kHz.

The boiling point of liquid nitrogen is $T_N = 77.36$ K. Since the shift of the resonant frequency was experienced, it can be asserted that the transition temperature belongs to the following interval: T $\in$ [77.36, 100] K.

Having verified the correct working of the apparatus developed so far, the next step was to mount the entire circuit into a NIM module.
Since the new configuration was very noisy, due to the presence of longer wires, some solutions were provided to get a cleaner signal. To reduce from the circuit signal the noise displayed on the oscilloscope, a T-junction splitter with a resistance value of 51 Ω was used. On the other hand, for the V_{AB} signal from the three-wire bridge, the noise was reduced using a lock-in amplifier, which is able to reduce a large amount of noise. The signal was controlled by a display and it was very stable.
Once the coil with the sample inside was inserted into the vacuum chamber, which was sealed with its own lid, the measurements were repeated with the new apparatus, to characterize it. The resulting curve is compared to the first one in figure 11.

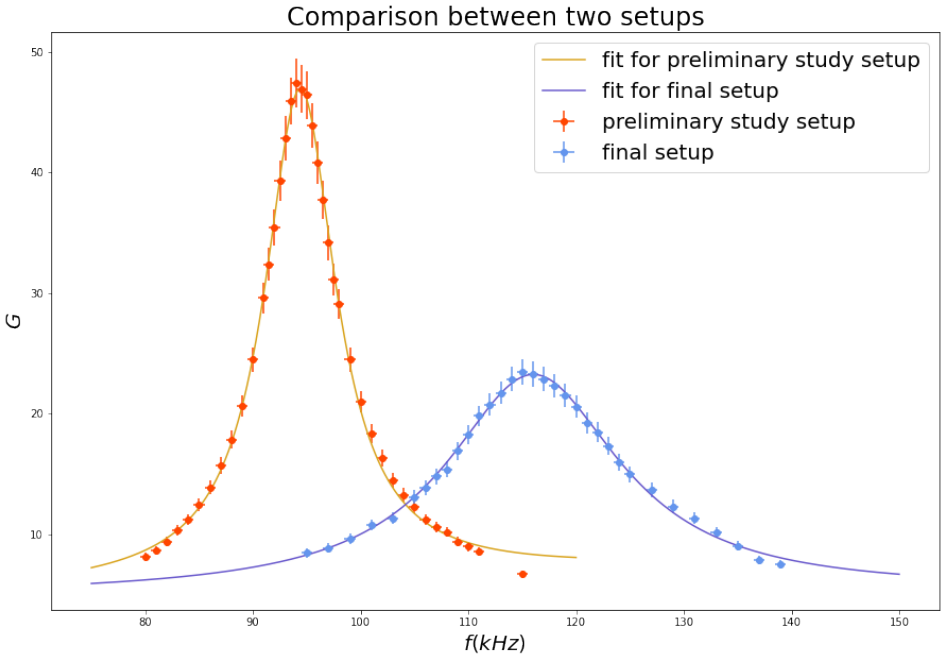

FIG. 11 Comparison between two different setups: the former (in orange) before mounting the final apparatus, the latter (in blue) after mounting the final setup.

With this new configuration, as it was expected, a lowering in the maximum value of the gain was found and the curve looks less narrow. This is a behaviour traceable to a change in resistance that has been already anticipated in the previous section, as there are longer wires with higher resistance. There is also a shift in the resonant frequency; this could be caused by several factors. One of them could be a change in the capacitance associated to the circuit. As a matter of fact, a parasitic capacitance might be present in the new setup, which has the effect of lowering the circuit capacitance. Another reason could be linked to the fact that the inductance of the coil may have been changed when inserted inside the sample holder. The presence of steel around the sample might provoke the change in the magnetic field lines. Thus the resonant frequency could have been varied because of the contribution of the inductance as well. The differences of the two configurations and a comparison with the theoretical expectations are listed in the table 2 below:

	f_0 (kHz)	Gain	r (Ω)	C (nF)	L (mH)
Theoretical	$\simeq 100$	$\simeq 100$	$\simeq 0$	$\simeq 4$	0.68 ± 0.04
Preliminary setup	94.39 ± 0.03	47 ± 3	11.8 ± 0.3	4.7 ± 0.3	0.60 ± 0.04
Final setup	116.02 ± 0.09	28 ± 2	28.3 ± 0.3	4.7 ± 0.3	0.40 ± 0.03
Final setup with fixed L				3.1 ± 0.6	0.60 ± 0.04

TAB. 2 Theoretical values of resonant frequencies, gains, wire resistances, capacities, inductances and experimental evaluations for different setups.

After having characterized the setup, the next step is to start the cooling process.
After sealing the lid of the vacuum chamber using a O-ring, a valve was slowly opened to gradually generate the vacuum. Once the pressure read from the Pirani gauge was stabilized, the cryocooler was switched on to start the cooling phase.
The behavior of the temperature during the cooling phase was studied in order to determine the cooling rate. The cooling rate obtained is equal to $v = -0.0319 \pm 0.0001$ K/s. Starting from an initial temperature $T_0 = 280.63 \pm 0.06$ K, it takes about 2 hours to reach a temperature of about 50 K. Data are shown in figure 12a. It should be underlined that after reaching lower temperatures, the acceleration of the cooling rate decreases, making the cooling process slower and the velocity lower.

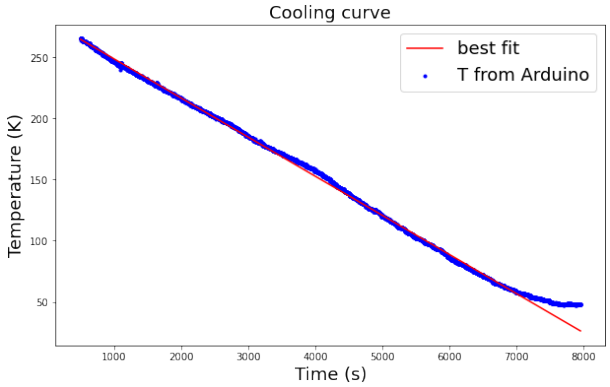

(a) Cooling curve of the sample holder, as a function of time. A linear fit was performed on the curve obtaining from the angular coefficient $m = -0.0319 \pm 0.0001$ the cooling rate. The intercept $q = 280.63 \pm 0.06$ indicates the room temperature.

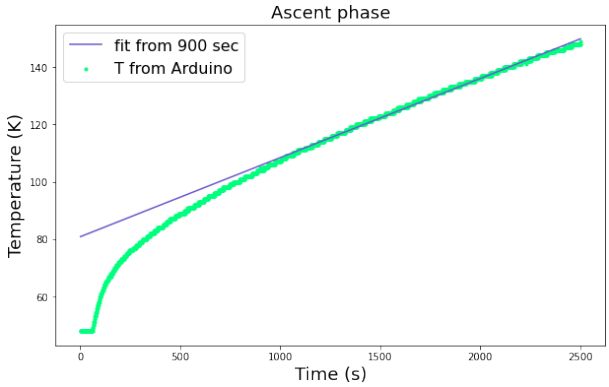

(b) Ascent phase described by a linear fit starting from 900 seconds. A linear fit was performed on the curve obtaining from the angular coefficient $m = 0.02769 \pm 0.00008$ K/s the heating rate.

FIG. 12 Characterization of the cooling setup.

The ascent phase started by switching off the cryocooler, without being helped from the heater. The curve is visible in fig 12b. The behaviour of the ascent phase is quite peculiar: as the machine stops (after some seconds in the graphic) the temperature rapidly increases, to again settle down in a linear trend described in figure by the fit. The ascent velocity is equivalent to the angular coefficient $v = 0.0275 \pm 0.0001$ K/s. Hence, to come back to room temperature, a time of almost two hours and a half is expected.

During the cooling phase, frequent measurements of the cold-finger temperature were made by sampling it thanks to the LabView program. At the same time it was possible to sample the temperature from the potentiometer as well. In this way it was possible to reconstruct the graph 13 below.

The plot shows the differences found between the temperature sampled from the two Pt100. There is a consistent discrepancy that reaches values of $\Delta t = 14$ K at 48 K of the cold finger. Therefore, the cooling velocity of the coil, which is $v_{coil} = 0.0284 \pm 0.0002$ K/s, is lower with respect to the one of the cold finger. This is reasonable since the first thermometer is tightly attached to it. As a result, its temperature will always be lower than the second one, since it is located close to the coil. Furthermore the latter could heat up due to the passage of current (Joule heating).

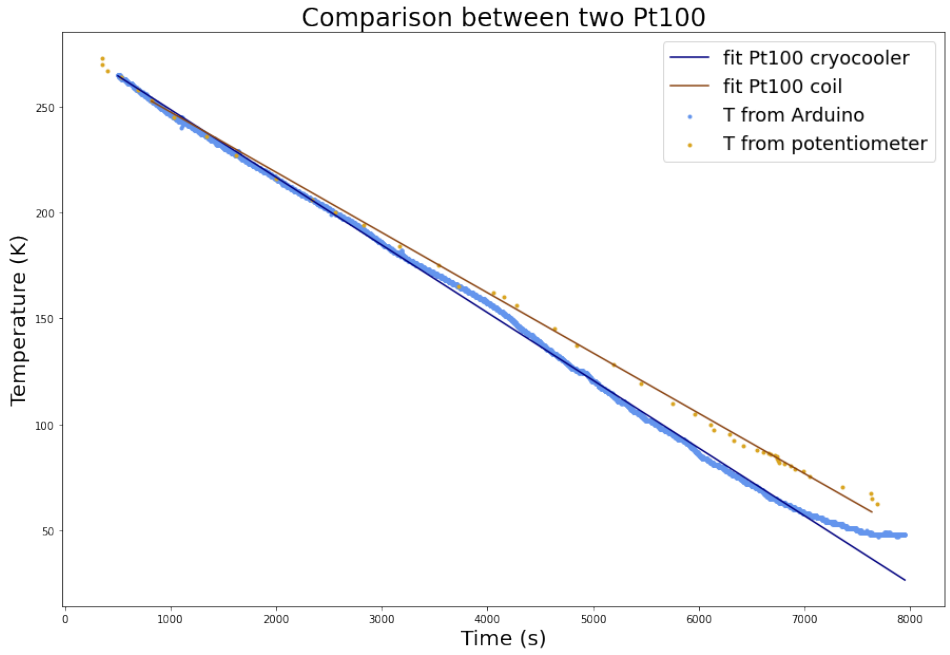

FIG. 13 A linear fit was performed on the curve obtaining from the angular coefficient $m = 0.02769 \pm 0.00008 K/s$ the velocity.

IV. DATA ANALYSIS

1. Measurement of the inductance

To evaluate the inductance, two pairs of resonance curves were plotted, respectively for the periods before and after reaching the superconducting condition. Every measurement is executed by reading V_{out} from the oscilloscope, changing the frequency related to the V_{in} signal in order to evaluate an estimate of the peak position.
These curves are shown in figure 14. At the top, the curves relating to the normal conductor condition are shown. Those were obtained when the cryocooler was still switched off. In this first case it was found a resonant frequency $f_0 = 115.91 \pm 0.06$ kHz and a maximum gain $G = 23.3 \pm 0.7$.
The curves obtained once the superconducting condition is reached are shown below. In particular, in the second set of measurements (14-*down,right*), the points have been taken to provide a much clearer view of the data around the peak (notice the frequency ranges chosen this time, during the data-taking process, compared to the ones of the (*down, left*) figure). It has a resonant frequency of $f_0 = 125.16 \pm 0.09$ kHz and a maximum gain of $G = 28.3 \pm 0.8$. For each of these curves the inductance has been calculated highlighting a lowering of this value when the superconductor condition is achieved. The values are shown in table 3 - *third column*.

		f_i (kHz)	r' (Ω)	L (mH)
Normal state	***first set***	115.85 ± 0.07	34.6 ± 0.3	0.40 ± 0.03
	second set	116.02 ± 0.09	34.9 ± 0.3	0.40 ± 0.03
Superconducting state	***first set***	125.4 ± 0.1	36.1 ± 0.3	0.34 ± 0.02
	second set	124.9 ± 0.1	36.5 ± 0.3	0.35 ± 0.02

TAB. 3 Resulting resonant frequencies, wire resistances and inductances are obtained by fitting the resonance curves.

Before and after the superconducting stage is reached, the gain has changed since there is a variation in the equivalent resistance R_{eq} of equation (10). The copper coil undergoes a shift in resistance, due to the lowering of the temperature[3]:

$$R_{50\,K} = R_0[1 + \alpha_0(T_{50\,K} - T_0)] \tag{14}$$

Where α_0 is the temperature coefficient of the copper resistance at *standard temperature*. The coil's resistance changes to the value of $R_{eq} = 1.3 \pm 0.4\ \Omega$. Therefore, exploiting again the equation (13) in order to evaluate the wires

resistance, using the new R_{eq}, the values found are displayed in table **3** - *second column*.
The mean shift in frequency of the transition is given by the difference between the weighted mean of the two resonant frequencies, found as: $\Delta f = 9.2 \pm 0.1$ kHz.

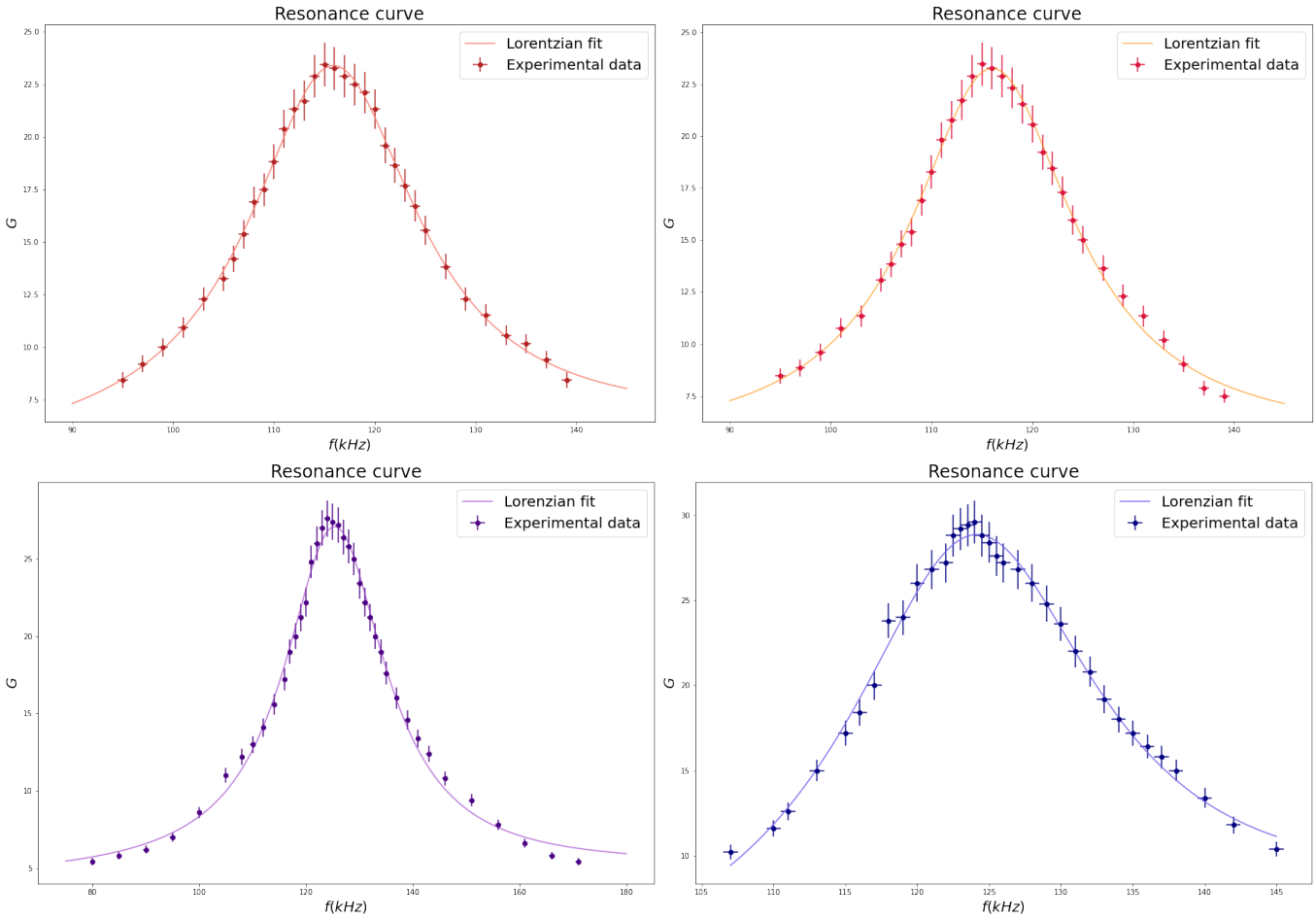

FIG. 14 Resonance curves obtained before and after reaching the superconducting condition.

2. Measurement of the critical temperature

To evaluate the critical temperature, which the sample becomes superconductor at, two more curves have been plotted. Pairs of values of resonant frequency and temperature in two different phases have been registered: in the cooling procedure and then the heating phase. These are shown in figure **15**.
The data were analyzed with a sigmoid function [4] to obtain the resonant frequency at the transition and the critical temperature of the sample when the system was cooled and heated. The sigmoid function is given by:

$$f_0(T) = \frac{f_1}{1 + exp(-\frac{(T-T_C)}{\tau})} + f_i \tag{15}$$

This function provides a good agreement with the obtained data. Going into more detail, the parameters appearing are:

- f_i: the initial resonant frequency;
- f_1: the difference between the final value of the resonant frequency, reached after the transition has occurred, and the initial value f_i;

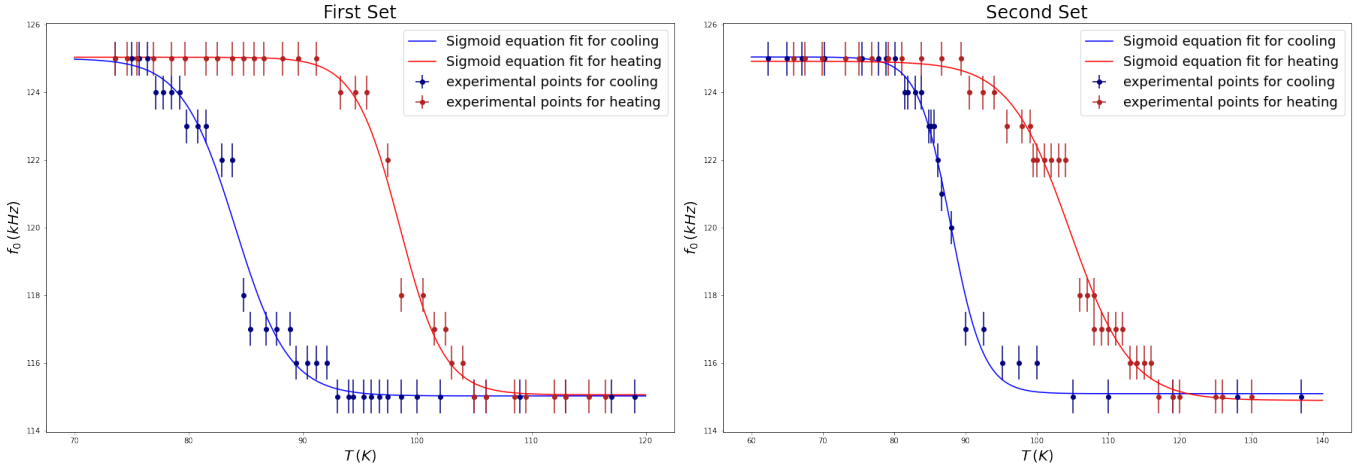

FIG. 15 Curves showing resonant frequency points as a function of temperature. The points related to the cooling phase are represented in blue, those related to heating phase in red. The two sets of points are fitted with a *sigmoid function* (15).

- T_C: the temperature corresponding to the bending of the curve, considered as the critical temperature at which the transition takes place;
- τ: a parameter that represents the temperature needed to raise the resonant frequency by a factor e.

The values found for these parameters are shown in the table 4.

		f_i (kHz)	$f_1 - f_i$ (kHz)	T_C (K)	τ (K)
First set	***cooling phase***	115.01 ± 0.05	125.0 ± 0.2	84.1 ± 0.2	2.3 ± 0.2
	heating phase	115.0 ± 0.2	125.0 ± 0.1	98.4 ± 0.2	2.0 ± 0.2
Second set	***cooling phase***	115.08 ± 0.06	125.1 ± 0.1	87.9 ± 0.2	2.3 ± 0.1
	heating phase	114.8 ± 0.2	124.9 ± 0.2	104.6 ± 0.4	4.2 ± 0.4

TAB. 4 Resulting initial and final resonant frequencies, critical temperatures and τ factor, obtained by fitting cooling and heating curves with the *sigmoid function* (15).

V. RESULTS AND CONCLUSIONS

A Wheatstone bridge was successfully built with a very stable output signal to evaluate the temperature second per second. The potentiometer matches perfectly the Pt100 resistance, and therefore a faithful balance was performed in every instant.
A selective amplifier was built to evaluate the inductance. The quality of the selection can be evaluated considering the quality factor of the resonant circuit, before and after the superconducting stage [5]:

$$Q = \frac{2\pi f_0 L}{R_{eq}} \tag{16}$$

With $R_{eq} = R_{coil} + r'$ the equivalent resistance that is involved in the RLC resonant circuit. In this way the selective amplifier bandwidth, that is the interval of frequencies allowed to pass, can be computed:

$$BW = \frac{f_0}{Q} \tag{17}$$

And all the results are displayed in table 5.
To improve the selectivity of the amplifier, the quality factor should assume a large value, and therefore R_{eq} should be very low. Since the wires resistance is not negligible and comparable to the resistance of the coil, it was difficult

	Q	BW (kHz)	*Interval* (kHz)
Normal state	6.5 ± 0.5	18 ± 1	$[98 \pm 1,\ 134 \pm 1]$
Superconducting state	7.0 ± 0.4	18 ± 1	$[107 \pm 1,\ 143 \pm 1]$

TAB. 5 Resulting initial and final resonant frequencies, critical temperatures and τ factor, obtained by fitting cooling and heating curves with a *sigmoid function.*

to achieve an higher quality factor. Thus it is reasonable to conclude that the bandwidth is acceptable within the experimental apparatus limits.

By plotting two pairs of resonance curves before and after the transition, the inductance of the coil was determined. As expected when the transition is reached, an increase in the value of the resonant frequency, related to the lowering of the coil inductance, is observed. The field lines are expelled from the coil and the inductance value drops going from a value $L_i = 0.40 \pm 0.03$ mH to $L_f = 0.35 \pm 0.02$ mH after the transition.

Analyzing the data relating to the resonant frequencies as a function of temperature, the range in which the critical temperature is located was determined for each set of data-taking processes:

$$set\ 1: \quad T_C \in [84.0,\ 98.4]$$

$$set\ 2: \quad T_C \in [87.9,\ 104.6]$$

Observing the figure **15** it is evident, for each set, the presence of hysteresis for the cooling and heating curves. This phenomenon could be firstly accounted to a lack of thermal equilibrium during the process, as the sample temperature is rapidly changing inside the vacuum chamber. Instead, assuming a thermal equilibrium condition for every single point (T, f_0) during the data taking, the biunivocal relation between temperature and resonant frequency, provided by the equation 15 holds. As a consequence of that, an overlap between the two curves of the two phases is expected. For this reason, the choice of the critical temperature T_C as the average value of the one displayed in tab. **4**-*third column* is not strict. As a result, it was assumed that the critical temperature should be within the intersection between the two intervals: $T_C \in [87.9,\ 98.4]$ K.

An intrinsic reason for the presence of hysteresis could arise from the fact that high temperature superconductors are type II classified, i.e. characterized by a mixed state with both microscopic superconducting regions and normal state ones. The traversing magnetic *flux tubes* are pinned to certain positions where the *pinning force* must be overcome in order to move them. Due to this *flux-pinning* the magnetic flux in the superconductor will not change in a reversible manner as the generated field changes, and the work needed to overcome this *pinning force* is connected with some losses in the superconductor [2],[9].
Furthermore, there are many different mathematical models explaining the hysteretic behaviour for type II superconductors.

The ceramic sample in analysis is either made of BSCCO or of YBCO. The BSCCO material owns two distinct crystalline superconducting phases. The 2212 phase ($Bi_2Sr_2CaCu_2O_9$) has a critical temperature of around 85 K. The 2223 phase ($Bi_2Sr_2Ca_2Cu_3O_{11}$) has a critical temperature of approximately 110 K[7]. The Yttrium based material has only one phase and the critical temperature is around 90 K[11], but it is sensible to the amount of oxygen present inside the compound, leading to a maximum of Tc = 95 K for x = 0.07 in $YBa_2Cu_3O_{7-x}$ [1].
Therefore we feel confident that the ceramic superconductor adopted in our experiment is YBCO.

1. Perspectives

Throughout the whole dissertation it was assumed for the inductance L a value which was calculated following the geometrical-based relation (11). However, this formula does not take into account the presence of the superconducting sample inside the coil, which could affect the final value of the inductance. Therefore, it is necessary to consider the

magnetic susceptibility χ of the material. From a theoretical point of view, the expression of the inductance for a filled coil becomes:

$$L = L_0(1 + \chi) \tag{18}$$

where L_0 is now the value previously calculated in relation (11).
In addition to that, it was considered the fact that the coil is not completely filled by the superconductor, hence it is convenient to introduce a parameter that quantifies the fraction v of occupied volume:

$$v = V_{\text{sample}}/V_{\text{coil}} \tag{19}$$

In this way it is possible to gain a more accurate estimate than the one in the (18). The final expression for the inductance will be then:

$$L = L_0(1 + v\,\chi) \tag{20}$$

It is possible to conclude that a direct measurement of the sample and the coil volumes, together with the knowledge of the susceptibility χ of the material would allow to evaluate better the inductance L.

VI. APPENDIX

1. Errors

A. Passive components

Passive components were measured using the RMS Digital Multimeter *Fluke 175* [6]. Therefore from the datasheet some parameters can be found to compute the error with the formula:

$$\delta_R = R \cdot p + dgt \cdot \delta_{least} \tag{21}$$

This means that for a quantity R the error is given by the product of the Reading and a percentage p given by the constructor, plus the product of the least significant digit on that scale δ_{least} and some integer-multiple *dgt*.

B. Oscilloscope measures

A fact needs to be highlighted: all the voltage measurements were read using the digital oscilloscope Tektronix TBS 1102B-EDU. The amplitude measurements read with the oscilloscope is always twice the real value, because it has a 51 Ω input resistor attached to the channels.

The errors associated for measurements in DC is[10]:

$$\delta V = \pm 3\%\, V \tag{22}$$

from 10 mV/div to 5 V/div, as the datasheet states.

The errors associated for measurements in AC is:

$$\delta V_{pp} = \delta V_{MAX} + \delta V_{MIN} \tag{23}$$

Therefore the waveform was always aligned to the horizontal axis.

C. Fit errors

The error on the parameters of a linear regression or a lorentzian fit is given by the standard deviation. It can be evaluated taking the square-root of the diagonal elements on the covariance matrix C. As an example, is reported here the case of the covariance matrix for a linear regression[8]:

$$C = \begin{bmatrix} \sigma_y^2 & 0 \\ 0 & \frac{\sigma_y^2}{\sigma_x^2} \end{bmatrix} \quad \text{with} \quad \sigma_x^2 = \frac{1}{N}\sum_{i=1}^{N}(x_i - \bar{x})^2,\ \sigma_y^2 = \frac{1}{N}\sum_{i=1}^{N}(y_i - \bar{y})^2 \tag{24}$$

where σ_x and σ_y are the standard deviations of the two parameters, N is the number of measurements and $\bar{x}$, $\bar{y}$ are the mean values of the x_i and y_i data.

REFERENCES

[1] Greenwood N.N. Earnshaw A. Chemistry of the elements. *Butterworth-Heinemann*, 2nd edition:1341, 02 1997.

[2] C. Navau A. Sanchez. Hysteresis loop and its relation to the critical current of finite superconducting cylinders. *Physica C*, 341-348:1441–1442, 2000.

[3] J.H. Dellinger. The temperature coefficient of resistance of copper. *Bulletin of the Boreau of standards*, vol. 7 No.1:71–72,

[4] Louis-S Bouchard et al. Detection of the meissner effect with a diamond magnetometer. *New J. Phys.*, 13 025017:8–10, 2011.

[5] T. L. Floyd. *Principles of Electric Circuits.* Pearson, 1981.

[6] Fluke. *True RMS Multimeters - User manual. Models 175, 177, 179*, 5 2003.

[7] P.K. Ahluwalia J. Kumar, D. Sharma and V.P.S. Awana. Enhanced superconducting performance of melt quenched bi2sr2cacu2o8(bi-2212). *Materials Chem. and Phys. 139*, 139:684, 11 2013.

[8] P. H. Richter. Estimating errors in least-squares fitting. *Communications Systems and Research Section*, TDA Progress Report 42-122:119–120, 08 1995.

[9] M. Sjostrom. *Hysteresis modelling of high temperature superconductors.*

[10] Tektronix. *Digital Storage Oscilloscopes - TBS1000B Series*, 1 2014.

[11] Sekitani T. Miura N. Ikeda S. Matsuda Y.H. Shiohara Y. Upper critical field for optimally-doped $yba_2cu_3o_{7-\delta}$. *Physica B: Condensed Matter.*, 319–324:6, 02 2004.